Uroporphyrinogen III Synthase Mutations Related to Congenital Erythropoietic Porphyria Identify a Key Helix for Protein Stability[†]

Arola Fortian,[‡,§] David Castaño,[‡] Gabriel Ortega,[‡] Ana Laín,[‡] Miquel Pons,[§] and Oscar Millet*[,‡]

Structural Biology Unit, CIC bioGUNE, Bizkaia Technology Park, Building 800, 48160 Derio, Spain, and Institute of Research in Biomedicine, Parc Científic de Barcelona, Josep Samitier 1-5, Barcelona, Spain

Received September 10, 2008; Revised Manuscript Received December 2, 2008

ABSTRACT: In the present study we have investigated deleterious mutants in the uroporphyrinogen III synthase (UROIIIS) that are related to the congenital erythropoietic porphyria (CEP). The 25 missense mutants found in CEP patients have been cloned, expressed, and purified. Their enzymatic activities have been measured relative to wild-type UROIIIS activity. All mutants retain measurable activity, consistent with the recessive character of the disease. Most of the mutants with a significant decrease in activity involve residues likely associated in binding. However, other mutants are fully active, indicating that different mechanisms may contribute to enzyme missfunction. UROIIIS is a thermolabile enzyme undergoing irreversible denaturation. The unfolding kinetics of wild-type UROIIIS and the suite of mutants have been monitored by circular dichroism. This analysis allowed the identification of a helical region in the molecule, essential to retain the kinetic stability of the folded conformation. C73R is found in one-third of CEP patients, and Cys73 is part of this helix. The integrated analysis of the enzymatic activity and kinetic stability data is used to gain insight in the relationship between defects in UROIIIS sequence and CEP.

Uroporphyrinogen III synthase (UROIIIS),[1] the fourth enzyme in the heme group biosynthetic route, catalyzes the rapid cyclization of the linear tetrapyrrole hydroxymethylbilane (HMB) to yield the asymmetric macrocycle uroporphyrinogen III (UROIII). One of the pyrrole moieties, the D ring, experiences an inversion of configuration during the enzymatic reaction (*1*). In the absence of UROIIIS this reaction competes with the fast degradation of HMB to produce the derivative uroporphyrinogen I (UROI) (*2*), which will not become a heme group because UROI is not a substrate for the subsequent enzymes in the biosynthetic route. An efficient inhibition of the enzyme by a spirolactamic derivative has led to the hypothesis that a spirocyclic pyrroline intermediate is formed in the course of the ring flip, a mechanism supported by recent quantum mechanical calculations on the conversion of HMB into UROIII (*3*).

A decrease in the enzyme activity produced by mutations is ultimately responsible for the human autosomal recessive congenital erythropoietic porphyria (CEP) (*4*). Genotyping of more than 110 CEP patients has identified 25 missense mutations (listed in Table 1) as well as 4 defects in the

Table 1: Specific Activity and Stability Values for the UROIIIS Mutants Related to CEP

mutant	frequency[a]	purification yield[b]/%	rESA[c]/%	E_a[d]/kcal·mol^{-1}
V3F	2	18.7	19.3 ± 2.8	113.0 ± 9.2
L4F	4	3.2	20.2 ± 1.2	100.3 ± 6.0
Y19C	1	16.2	13.1 ± 2.2	63.4 ± 8.2
S47P	6	1.7	100.0 ± 1.1	96.0 ± 4.3
P53L	3	0.0	na	na
T62A	1	27.7	1.2 ± 0.1	27.7 ± 0.8
A66V	1	54.8	95.6 ± 0.2	32.0 ± 2.6
A69T	5	13.6	24.4 ± 1.3	42.1 ± 6.8
C73R	31	4.4	14.5 ± 1.2	22.0 ± 9.5
E81D	1	39.4	100.0 ± 3.0	87.0 ± 4.4
V82F	1	26.3	93.8 ± 1.8	87.0 ± 0.6
V99A	4	9.4	88.2 ± 5.1	103.4 ± 6.0
A104V	1	23.0	60.6 ± 3.7	91.5 ± 2.3
I129T	2	1.9	20.0 ± 4.0	67.8 ± 1.4
H173Y	2	4.0	72.6 ± 1.4	33.0 ± 0.9
Q187P	1	1.2	15.0 ± 1.9	71.1 ± 2.5
G188R	2	2.2	41.4 ± 7.6	78.9 ± 7.8
G188W	1	2.3	31.6 ± 4.3	78.7 ± 3.2
S212P	3	8.3	20.0 ± 4.1	33.6 ± 2.4
I219S	2	3.0	85.0 ± 5.0	40.0 ± 1.1
G225S	5	26.6	32.4 ± 10.2	92.0 ± 4.8
T228M	3	54.8	97.5 ± 2.5	95.7 ± 3.4
G236V	1	5.8	34.0 ± 3.9	44.2 ± 1.8
L237P	2	2.8	57.9 ± 2.2	46.7 ± 9.0
P248Q	8	2.5	29.2 ± 3.2	86.2 ± 5.5

[a] Compiled from all of the case studies reported in the literature. [b] Recombinant protein purification yield, referred to wild-type UROIIIS. [c] Referred to the wild-type UROIIIS specific activity. Errors have been estimated from duplicate measurements. [d] Value for wild type: 101.5 kcal·mol^{-1}. Errors have been estimated from the linear fitting of the kinetic rates versus temperature.

[†] Support was provided from The Department of Industry, Tourism and Trade of the Government of the Autonomous Community of the Basque Country (Etortek Research Programs 2005/2007), from the Innovation Technology Department of the Bizkaia County, from the Ministerio de Ciencia y Tecnología (CTQ2006-09101/BQU, CSD2008-00005, and BIO2007-63458), an Institute for Research in Biomedicine fellowship to A.F., and from the Ramon y Cajal program.

* Corresponding author. Phone: 34 944 061 300. Fax: 34 944 061 301. E-mail: omillet@cicbiogune.es.

[‡] CIC bioGUNE.

[§] Parc Científic de Barcelona.

[1] Abbreviations: CEP, congenital erythropoietic porphyria; UROIIIS, uroporphyrinogen III synthase; HMB, hydroxymethylbilane; UROIII, uroporphyrinogen III; UROI, uroporphyrinogen I; rESA, residual enzyme specific activity; PBGD, porphobilinogen deaminase; CD, circular dichroism; E_a, activation energy barrier; NMR, nuclear magnetic resonance spectroscopy.

10.1021/bi801731q CCC: $40.75
Published on Web 12/19/2008

promoter region (*4, 5*). The distribution of mutants among patients is quite homogeneous (with a mean value of two patients per mutation) except for C73R that is present in about one-third of the total reported cases (see Table 1) (*6*). The phenotype of the pathology varies extensively among patients, but common symptoms include hemolitic anemia produced by the decreased heme levels, scars, and bullous lesions generated by the accumulation of UROI or its derivatives in the body and skin photosensitization caused by the photoreactive nature of the accumulated precursors (*7*−*12*). In principle, the severity of the pathology should be related to the residual enzyme activity, reported in the literature for some of the deleterious mutants. Although this relationship holds qualitatively, no correlation between such values and the phenotype has been found, to some extent because most of the activity values reported to date are referred to the expressed yield in *Escherichia coli* (*4*).

In diseases related to protein malfunction, it is diagnostically and therapeutically essential to understand the multiple mechanisms that relate the specific mutants with the pathology. An inherited mutation can alter protein function in very different ways. Alterations in the coding DNA can destabilize the corresponding mRNA to decrease the protein expression in the cell. At the protein level, some of the defects may alter the catalytic machinery of the enzyme, whereas other mutations can undermine the stability of the folded conformation. The latter is of particular importance since UROIIIS is a thermolabile enzyme (*13*) undergoing slow irreversible denaturation (*14*−*16*). Studies of the changes in stability introduced by a deleterious mutation are sometimes characterized by semiquantitative experiments (i.e., pulse−chase assays or treatments with chemical agents) (*17*). However, an accurate thermodynamic treatment is much less common. When irreversible denaturation occurs, the stability of the folded conformation is controlled by the unfolding kinetics (kinetic stability) (*18*). In the present study we have employed circular dichroism to investigate the unfolding kinetics of purified wild-type human UROIIIS and all of the missense UROIIIS mutants reported to produce CEP. Enzyme activity assays have been described (*19, 20*), and we have also measured the specific activity (activity per milligram of purified enzyme) with respect to wild-type UROIIIS using purified proteins (rESA). This in vitro approach corrects for the very different expression levels observed among the mutants. An integrative analysis of the information provided by the large set of mutants studied has identified protein regions prone to become destabilized upon mutation and has provided an explanation for the high clinical severity found in CEP patients carrying the C73R mutation.

EXPERIMENTAL PROCEDURES

Subcloning and Site-Directed Mutagenesis. pHTU3S plasmid containing the gene codifying for UROIIIS was provided by Prof. J. Phillips (Utah University). To obtain UROIIIS mutants, site-directed mutagenesis employed the commercial QuickChange II kit (Quiagen) with custom-made oligonucleotides as PCR reaction primers (Invitrogen). Primers designed for the polymerase chain reaction reproduce codon mismatches found in CEP patients. A table with the primers used in the reaction is included in the Supporting Information. Human porphobilinogen deaminase (PBGD), required for the UROIIIS specific activity assay (*20*), was amplified by PCR reaction using the forward and reverse primers 5′-ACACCATGGCATCTGGTAACGGCAATGCGGCTGCAACGGCGG-3′ and 5′-GGGGAAGCTTTTAATGGGCATCGTTAAGCTGC-3′ and cloned into a pETM-11 expression vector using the *Hin*dIII and *Nco*I restriction sites.

Protein Sample Preparation. Freshly transformed *E. coli* BL21(DE3) cells were used for protein expression. UROIIIS (MW 31.1 kDa) has been purified employing the following protocol: the cell pellet (1 L of culture) is resuspended in 20 mL of buffer A (20 mM sodium phosphate, 500 mM NaCl, 5 mM imidazole, pH 7.4) and thoroughly sonicated. The supernatant is mixed with 3 mL of His-tag resin (Ni-NTA; Invitrogen) and eluted with buffer A containing 500 mM imidazole. Protein is further purified by size exclusion chromatography (Superdex 75; GE Healthcare) under isocratic conditions (20 mM Tris, 150 mM NaCl, pH 8.0). PBGD (MW 42.6 kDa) is purified following the same protocol except that the gel filtration chromatography uses a Superdex 200 column (GE Healthcare), eluted in 20 mM Tris and 150 mM NaCl at pH 7.0. All of the purification protocols proceeded at 4 °C to minimize proteolysis, and samples were concentrated up to 5 μM and also stored at 4 °C. Protein concentration was measured by UV spectrophotometry at 280 nm, employing extinction coefficients of 25410 and 15970 $M^{-1}\cdot cm^{-1}$ for UROIIIS and PBGD, respectively (*21*). Between 0.5 and 1.2 mg of pure wild-type UROIIIS and 3.8 mg of PBGD were obtained per liter of culture.

UROIIIS Enzymatic Assay. The determination of UROIIIS specific activity is based on the method developed by Jordan and modified by Tsai et al. and Hart and Battersby (*20, 22, 23*). Since the natural substrate for UROIIIS is very unstable, the assay starts with porphobilinogen (Frontier Scientific) that is enzymatically converted into UROIII by the tandem action of PBGD and UROIIIS. Porphobilinogen (50 μL of a 2 mM solution) is first mixed with 20 μL of PBGD (150 μM) and 145 μL of 20 mM Tris and 150 mM NaCl at pH 8.0. After 1 min, 50 μL of UROIIIS (5 μM) is added. Some spontaneous formation of UROI is also expected. Reaction is stopped after 1 min by freezing the sample in liquid nitrogen. Uroporphyrinogens are then oxidized to uroporphyrins by adding I_2 in KI. The excess of iodine is removed with sodium metabisulfite (saturated solution), and the protein is precipitated by lowering the pH with trichloroacetic acid (10% w/v). Supernatant is diluted in 0.1 M HCl. Uroporphyrin III and uroporphyrin I are separated by high-performance liquid chromatography (HPLC) as previously described (*20, 24*). The specific activity of the mutant proteins is measured *immediately* after purification in parallel with a fresh sample of wild-type UROIIIS. The relative enzymatic specific activity (rESA) is obtained by comparing the UROIII peaks for the mutant and the wild type in the chromatogram. Activity is reported as a percentage of the wild-type value, and at least two duplicates were used to account for the experimental error.

Circular Dichroism Measurements. All experiments were collected in a JASCO J-810 spectropolarimeter, using a quartz cuvette of 0.2 cm path length. Sample concentration was 5 μM for all of the tested proteins. The isothermal unfolding rate (k_{NU}) was determined for each of the UROIIIS mutants at, at least, four different temperatures (in the range:

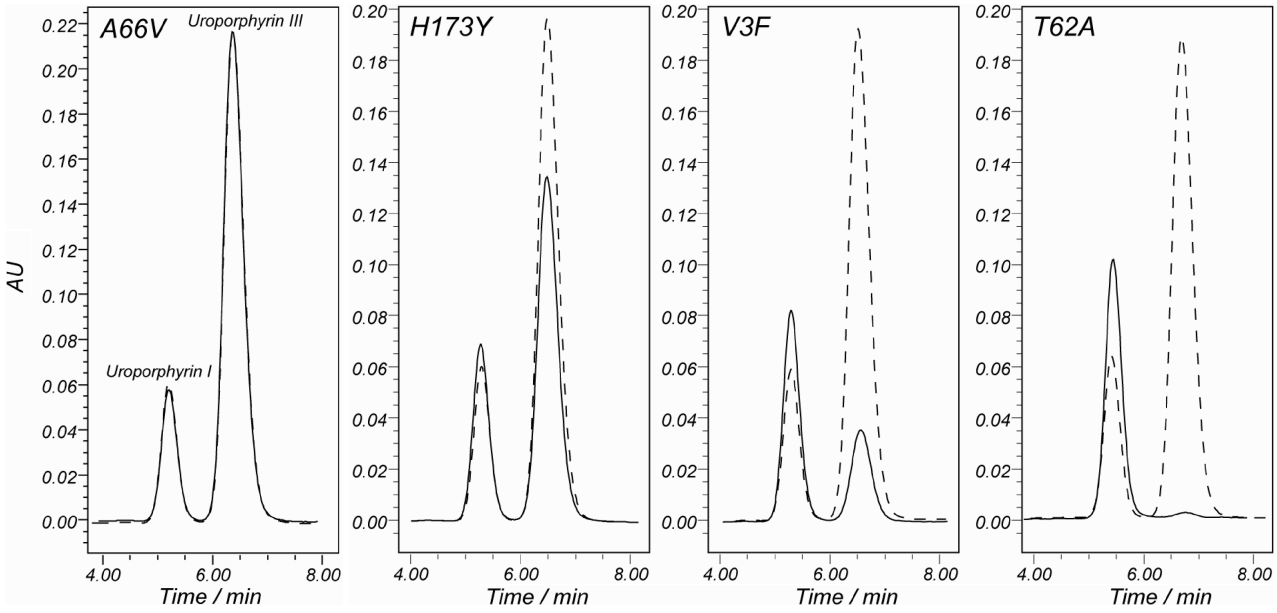

FIGURE 1: HPLC separation of uroporphyrin I (retention time: 5.3 min) and uroporphyrin III (retention time: 6.5 min) for four representative mutants. Solid and dashed lines correspond to the mutant and the wild-type chromatograms, respectively.

37−52 °C) whereas seven different temperatures were used to characterize the wild-type one (37, 40, 42, 44, 46, 48, 50 °C). Freshly purified samples at 4 °C were transferred to the spectropolarimeter, prestabilized to the target temperature, and maintained at constant temperature until the decay reached a plateau. Typical decay times lasted from 2 h (at 50 °C) to 3 days (at 41 °C), but differences were observed depending on the activation energy barrier (E_a). The time constant was extracted from the decay over time of the signal at 222 nm.

Apparent melting temperatures were measured using temperature scans from 10 to 75 °C to ensure the proper determination of the baselines in both the folded and unfolded states. Data were analyzed using in-house built scripts programmed in Matlab (Simulink) assuming the linear extrapolation method (*25*): the molar ellipticity at each point of the transition can be described as a linear combination of the expected values for the folded (θ_F) and unfolded (θ_U) states. The values for θ_F and θ_U are obtained from extrapolations of the linear baselines. Thermal melts for wild-type protein were repeated at four different scan rates (1, 2, 3, and 4 °C/min).

NMR Experiments. A 50 μM sample of wild-type UROIIIS was used. NMR data were collected in a Bruker Avance III, 600 MHz spectrometer at 37 °C. Each experiment employed WATERGATE solvent suppression (*26*) and had a duration of 20 min with a total experiment time of 3 days.

RESULTS

Expression, Purification, and Determination of the Specific Activity for the 25 Mutants in UROIIIS Related to CEP. UROIIIS missense mutants reported in the literature (*4, 9−12, 27−29*) span throughout the enzyme with only two mutants originating at the same amino acid (G188R and G188W) (*7, 30*). Wild-type UROIIIS and the 25 point mutants were expressed in *E. coli* and isolated with a final purity beyond 97% as determined by SDS gel electrophoresis (some examples are shown in the Supporting Information). The yields of pure protein for the different mutants, relative to wild-type UROIIIS, are listed in Table 1. All proteins showed a reduction in the amount of protein compared to wild-type UROIIIS, with yields spanning from 1.2% to 55%. In the case of P53L no expression could be detected, consistent with previous reported attempts (*31*). The decrease in the yield can be caused by codon alteration at the DNA level or by changes in the physicochemical properties of the protein (for instance, a decrease in the resistance to become proteolyzed or a reduction in the chelating properties of the mutated enzyme).

The specific activity was measured for all of the expressed mutants following a previously described method (*20*) (see Experimental Procedures). Figure 1 shows the HPLC chromatogram for four representative mutants. Uroporphyrin III and uroporphyrin I are eluted at 6.5 and 5.3 min, respectively. The traces corresponding to mutant and wild-type UROIIIS are represented in Figure 1 with solid and dashed lines, respectively. Large differences can be observed among the mutants: whereas the chromatograms corresponding to A66V and wild type overlap almost perfectly, much less UROIII is produced by T62A. The amount of UROI produced increases when the specific activity is reduced, an observation already reported in the literature (*20*). The relative specific activities (rESA) for the full mutant set are listed in Table 1. To our knowledge, these measurements constitute the most comprehensive functional analysis of UROIIIS mutants. The effects of mutants producing CEP are often reported in the literature as "expressed enzymatic activity" (*4*) that should be proportional to the purification yield times rESA. Our results clearly indicate that the very low expressed activity values (often close to zero) are mainly due to a drop in the expression (and purification) yield instead of alterations in the specific activity of the mutant.

The UROIIIS mutant set presents a large variability in the rESA, with values ranging between 1.2% and 100%. Ten out of 25 mutants (V3F, L4F, Y19C, T62A, A69T, C73R, I129T, Q187P, S212P, and P248Q) show a significant drop in specific activity with values below 30%. Most of these

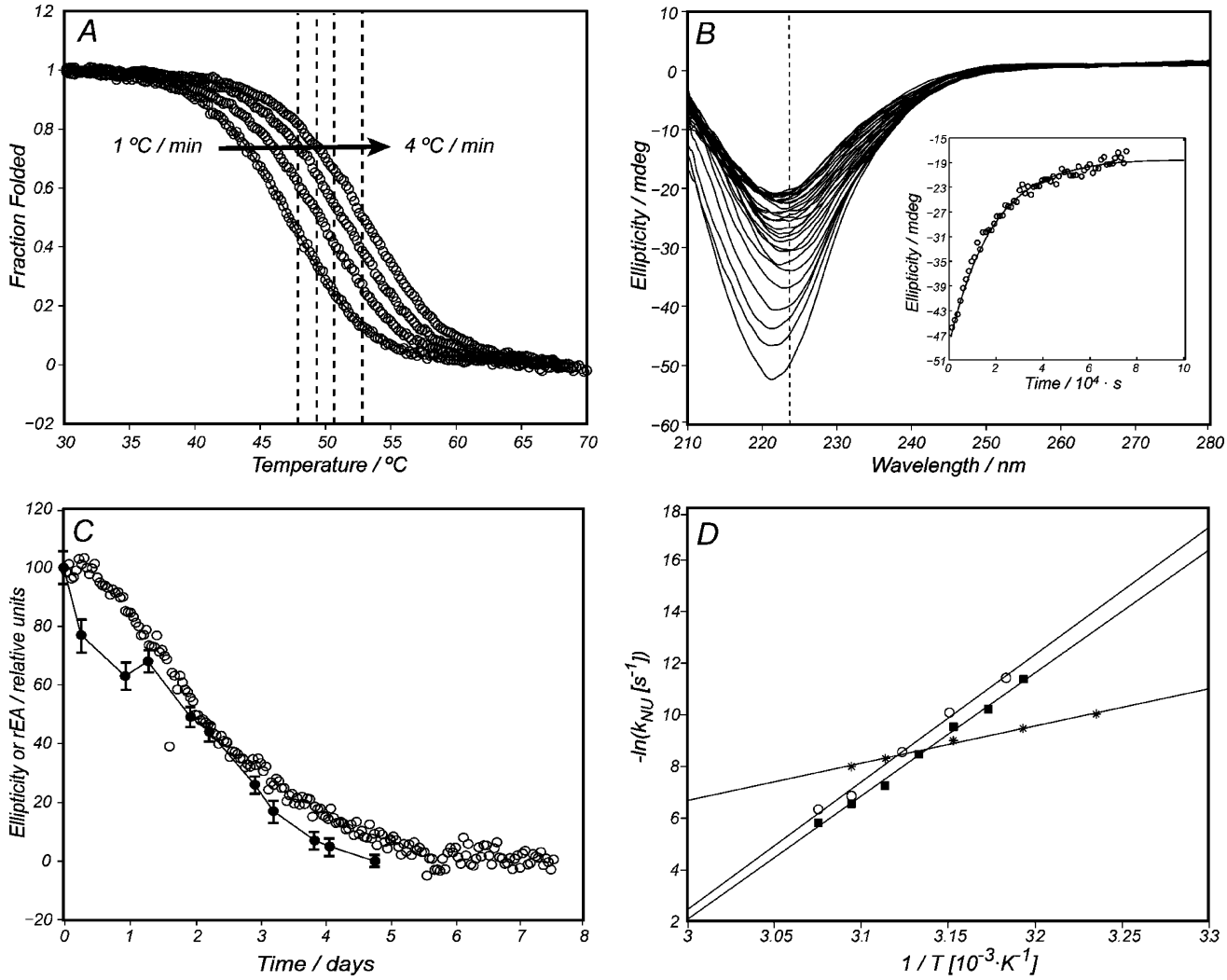

FIGURE 2: (A) Thermal denaturation melting curves for wild-type UROIIIS at varying scanning rates (1−4 °C/min). The temperature at mid-denaturation (T_m) is marked by dashed vertical lines at each scanning rate. (B) Circular dichroism spectra showing the signal decay over time for wild-type UROIIIS at 41 °C. The ellipticity at 222 nm has been used to calculate the decay rate constant from nonlinear fitting (inset). (C) Decays over time for the ellipticity (open circles) and the specific activity (rEA, filled circles) at physiological temperature in a sample of wild-type UROIIIS (5 μM). The polygonal line is added only to help the eye. (D) Arrhenius plots for unfolding transitions of UROIIIS as measured with CD spectroscopy: wild type (black squares), S47P (open circles), and A66V (asterisks). The lines represent the linear regression of the data, used to obtain the activation energy (E_a, listed in Table 1).

residues have been identified as putative substrate binders in an NMR chemical shift perturbation experiment (*32*), and they probably belong to the active site, offering an explanation for their loss in activity upon mutation. On the opposite side, seven mutants giving a CEP phenotype (S47P, A66V, E81D, V82F, V99A, I219S, and T228M) show a relative specific activity of 85% or more, suggesting a different mechanism to produce the enzyme malfunction. Our hypothesis is that mutants can also alter protein unfolding thermodynamics, and therefore, the stability properties of UROIIIS have been investigated.

Wild-Type UROIIIS Is a Kinetically Stable Protein. The thermal denaturation of wild-type UROIIIS has been investigated by circular dichroism (CD). The temperature where half the protein is unfolded (T_m) is the most common parameter to define protein thermal stability (*33*). However, as shown in Figure 2A, the apparent T_m values depend on the scanning rate, suggesting the presence of an irreversible denaturation process (*34, 35*). The isothermal unfolding kinetics of UROIIIS has been measured by CD at different temperatures. Figure 2B,C shows the exponential decay of the ellipticity at 37 °C (open circles). The relative decrease in ellipticity parallels the loss of specific activity (closed circles in Figure 2C). The decrease in the CD signal shown in Figure 2B can be characterized by an apparent kinetic rate (k_{app}; see inset).

The simplest model that explains UROIIIS denaturation is the three-state model, previously used to describe the so-called "kinetically stable proteins" (*15*):

$$N \underset{K_{UN}}{\overset{K_{NU}}{\rightleftharpoons}} U \xrightarrow{K_{UF}} F$$

where N is the native state and U the unfolded state that spontaneously converts into the more stable (often inactive) final state F. Dynamic light scattering measurements and optical inspection of samples incubated over time revealed the formation of protein precipitates, indicating that the F state is an aggregate form of UROIIIS. The kinetic rates k_{NU}, k_{UN}, and k_{UF} are related to the conversion processes indicated by the arrows. The apparent rate k_{app} takes the general form (*34*):

$$k_{app} = \frac{k_{NU}k_{UF}}{k_{UN} + k_{UF}} \quad (1)$$

When k_{UF} is much larger than k_{UN}, the apparent rate is equivalent to the unfolding rate ($k_{app} \approx k_{NU}$) (*16*). Two observations support the use of this approximation in the case of UROIIIS. (i) k_{app} is concentration independent, within experimental error, in the explored range (5−50 μM). Thus, k_{app} is monitoring a *unimolecular* event of spontaneous unfolding instead of the *multimolecular* transition to F. (ii) The disappearance of the native species, followed by NMR, results only in a decrease in intensity, without changes in the spectral pattern that could indicate the presence of nonaggregated unfolded forms. All together, it can be concluded that the unfolding process is the limiting step for UROIIIS with no significant accumulation of the unfolded state at concentrations over 5 μM.

At physiological temperature, k_{NU} is equal to (1.6 ± 0.2) × 10^{-6} s^{-1} for wild-type UROIIIS, corresponding to a half-life time of 61.1 h. We have explored the temperature dependence of the unfolding rate constant in a range between 37 and 50 °C. These data have been analyzed collectively assuming the Arrhenius model:

$$k_{NU} = Ae^{-E_a/RT} \quad (2)$$

where E_a is the enthalpic contribution to the activation energy and A is the frequency factor, which includes the entropic contribution. The activation energy for wild-type UROIIIS, derived from the slope of the linear plot of ln(k_{NU}) versus 1/T (black squares in Figure 2D) is 101.5 kcal·mol^{-1}. E_a is the enthalpy difference between the active folded conformation (N state) and the highest energy conformation in the path toward unfolding. For wild-type UROIIIS this barrier is large, falling in the range of values for proteins that experience kinetic stability (*16*). As a test of consistency for the Arrhenius model, the obtained E_a value has been used to predict the dependence of T_m with the scanning rate in the temperature denaturation experiments (*36, 37*) shown in Figure 2A (see Supporting Information). The good agreement between experimental and calculated data validates the use of this model to characterize UROIIIS unfolding kinetics.

Destabilizing Regions in UROIIIS. To evaluate the impact of the CEP-associated mutations in the stability of UROIIIS, we have determined the unfolding rate constants for the mutants at a minimum of four temperatures (in range: 34−52 °C). The half-lifes at 37 °C range from 0.16 to 339 h, and the changes in the unfolding rate, relative to wild type, are shown in Figure 3A. Linear plots between ln(k_{NU}) and 1/T are obtained for all of the mutants (two representative examples are shown in Figure 2D), allowing an estimation of the activation energy barriers for the entire mutant set, listed in Table 1 and also shown in Figure 3B. Whereas the majority of the mutants cause only small perturbations in the activation energy barrier, a subset of them decrease the unfolding energy barrier by at least a factor of 2.

Figure 4 shows a ribbon diagram of wild-type human UROIIIS (*38*) with the mutated positions highlighted and

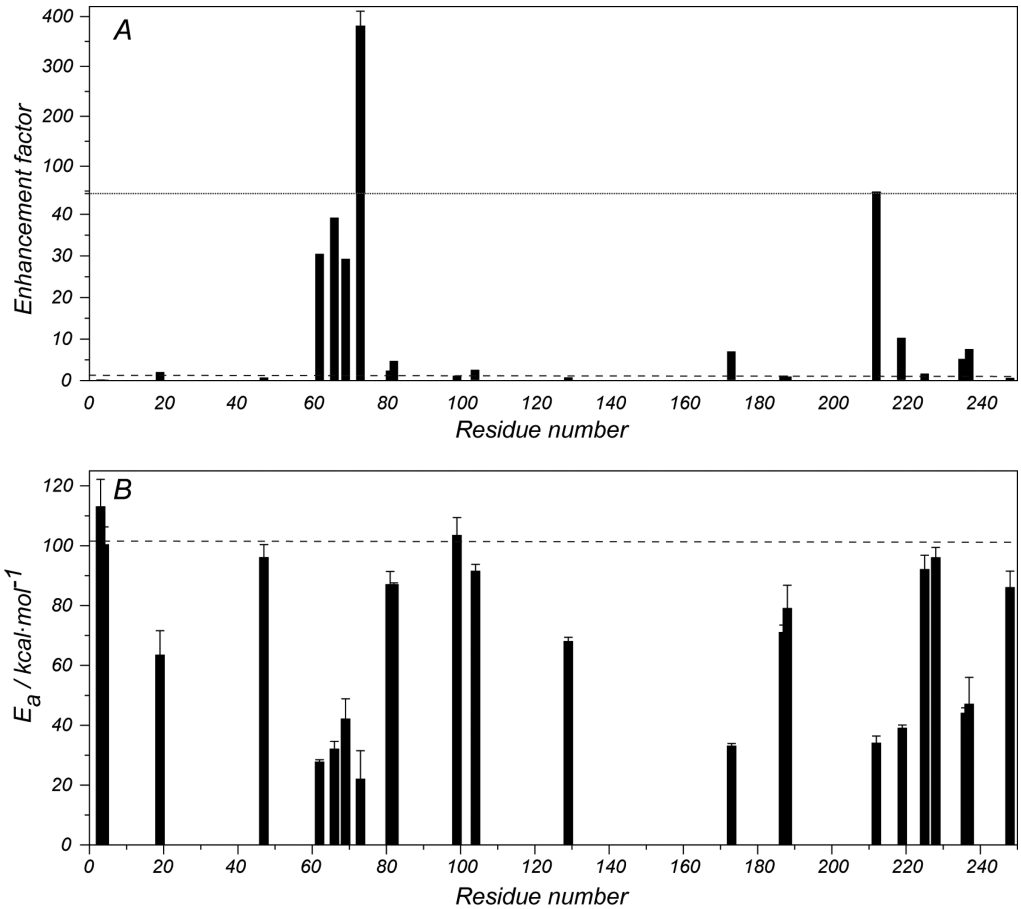

FIGURE 3: (A) Enhancement factor (k_{NU}(Mut)/k_{NU}(WT)) calculated at 37 °C for each of the mutants. There is a change in the ordinate scale, indicated by the dotted line in the center of the panel. (B) Activation energy (E_a) as a function of the residue number. The dashed lines indicate the magnitude values for wild type.

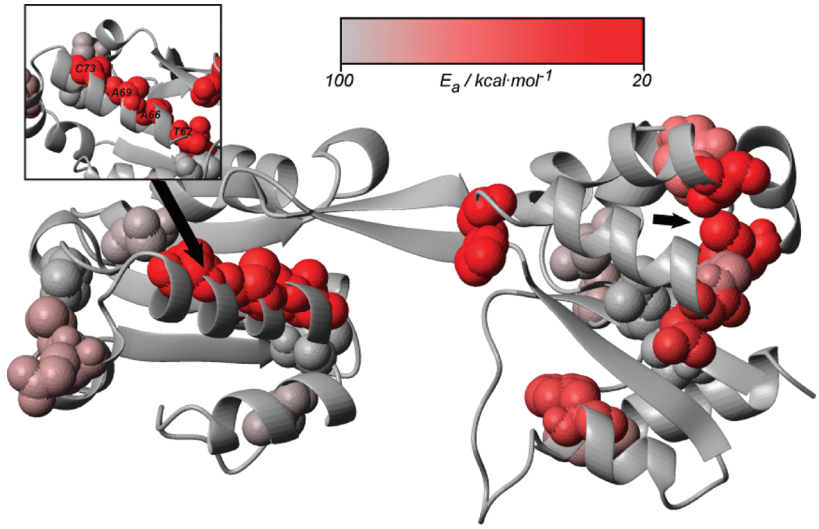

FIGURE 4: Ribbon representation of wild-type human UROIIIS (PDB code 1jr2) (*38*). Residues considered in the present study are highlighted by CPK representation. Color code reflects the obtained activation energy value upon mutation according to the legend displayed in the figure. The arrows pinpoint the regions of the protein prone to become destabilized upon mutation. A different view of the third helix of the N domain is also shown in the inset.

color coded to display the E_a values. Mutants of residues belonging to the third α-helix of the N domain result in a significant increase in the unfolding rate at 37 °C, accompanied by a large decrease in the activation energy barrier. C73, whose mutation to arginine is the most frequently found in CEP patients (*4*), belongs to this helix. The C73R mutation causes the largest increase in k_{NU}, with an unfolding rate at 37 °C 380 times faster than wild-type UROIIIS, although the E_a for C73R parallels activation energies from other destabilizing mutants (within experimental error).

A second cluster with large destabilizing effects upon mutation can be identified in the region between S212 and I219 (indicated by an arrow in Figure 4).

DISCUSSION

In the present study we have determined the specific activity for all of the missense UROIIIS mutants found in CEP patients to date. The obtained values, measured using purified recombinant protein, are much larger than the previously reported expressed enzyme activities and are poorly correlated with the severity of the CEP phenotype. Actually, the rESA values measured for the mutant set vary from 1.2% to 100% with an average value of 50.3%. These high values are in good agreement with the recessive character of the disease: a person carrying a single mutated allele would still retain between 50.6% and 100% of the total specific activity. Most of the pathogenic mutants with an specific activity less than 30% are located in residues that may bind to the substrate, according to a previous NMR chemical shift perturbation analysis (*32*). These residues span throughout the protein, supporting the idea that the catalytic site occupies the cleft between the two domains.

UROIIIS suffers irreversible denaturation with time in purified form. Here we demonstrate that the folded conformation is not stable at physiological temperature and undergoes spontaneous unfolding followed by aggregation. Protein unfolding is drastically accelerated in a subset of mutants that retain most of the synthase activity (A66V, H173Y, I219S, and L237P), providing an explanation for their CEP phenotype. A comparison of the activation energy barriers for unfolding of the different mutants has identified two regions where mutations cause significant increases in the unfolding rate: residues 212 and 219 in the C-terminal region and, especially, the third helix of the N-terminal domain. Mutated residues found in CEP patients with severe symptoms (T62A, A66V, A69T, C73R) are located in the same face of the helix and interconnected by a spine of hydrogen bonds (see Figure 4). C73R is a hot-spot mutation found in more than one-third of the CEP patients and the one causing the most severe phenotype (*4*). Moreover, this mutation is panethnic, not being produced by dispersion from a single ancestor (*39*). Unfolding kinetic analysis revealed that C73R becomes the most destabilizing mutation in UROIIIS with the lowest E_a value, resulting in an unfolding rate 380 times faster than wild-type UROIIIS. The residual specific activity for the enzyme is low but not null (14.5% *in vitro*), offering an explanation for the viability of the homozygous genotype (C73R/C73R), found in some severely affected cases of CEP.

A mutant subset (S47P, E81D, V82F, V99A, A104V, and T228M) retains very high synthase activity and shows no decrease in stability. S47P is the CEP-associated mutant closest to wild type according to our analysis. It is found only in mild CEP patients, being the only reported case of homozygotic mutation in UROIIIS carried by a healthy individual (*27*). E81D and V82F have been reported to produce impaired splicing at exon 4 to generate a truncated version of the protein in the cell (*4*). All of the other mutants from this group have always been found accompanying mutants related to more severe symptoms (V99A/C73R, A104V/C73R, T228M/C73R, T228M/G225S) (*8, 31, 40*), suggesting that these mutations may just be gene polymorphism probably also present in healthy individuals.

In conclusion, in the present study we have measured the relative enzymatic activities and the unfolding kinetics of wild-type UROIIIS and all 25 mutants found in CEP patients. Kinetic stability varies widely among the tested enzyme mutants, offering a plausible mechanism to explain pathogeneity for the mutants that retain full specific activity. The

identification of a novel region, essential for the stability of the protein, offers an explanation for the large effect of C73R found in one-third of patients.

ACKNOWLEDGMENT

We are indebted to Prof. John Phillips (Utah University) for providing us with the plasmid containing the human UROIIIS gene. A.F. and D.C. equally contributed to the work.

SUPPORTING INFORMATION AVAILABLE

A table containing the primers used to obtain the 25 UROIIIS mutants, a figure showing an SDS gel of purified proteins, and a consistency test for the Arrhenius model used to calculate the activation energy barriers. This material is available free of charge via the Internet at http://pubs.acs.org.

REFERENCES

1. Schubert, H. L., Raux, E., Matthews, M. A., Phillips, J. D., Wilson, K. S., Hill, C. P., and Warren, M. J. (2002) Structural diversity in metal ion chelation and the structure of uroporphyrinogen III synthase. *Biochem. Soc. Trans. 30*, 595–600.
2. Battersby, A. R. (2000) Tetrapyrroles: the pigments of life. *Nat. Prod. Rep. 17*, 507–526.
3. Silva, P. J., and Ramos, M. J. (2008) Comparative density functional study of models for the reaction mechanism of uroporphyrinogen III synthase. *J. Phys. Chem. 112*, 3144–3148.
4. Desnick, R. J., and Astrin, K. H. (2002) Congenital erythropoietic porphyria: advances in pathogenesis and treatment. *Br. J. Haematol. 117*, 779–795.
5. Stenson, P. D., Ball, E., Howells, K., Phillips, A., Mort, M., and Cooper, D. N. (2008) Human Gene Mutation Database: towards a comprehensive central mutation database. *J. Med. Genet. 45*, 124–126.
6. Stenson, P. D., Ball, E. V., Mort, M., Phillips, A. D., Shiel, J. A., Thomas, N. S., Abeysinghe, S., Krawczak, M., and Cooper, D. N. (2003) Human Gene Mutation Database (HGMD): 2003 update. *Hum. Mutat. 21*, 577–581.
7. Shady, A. A., Colby, B. R., Cunha, L. F., Astrin, K. H., Bishop, D. F., and Desnick, R. J. (2002) Congenital erythropoietic porphyria: identification and expression of eight novel mutations in the uroporphyrinogen III synthase gene. *Br. J. Haematol. 117*, 980–987.
8. Xu, W., Warner, C. A., and Desnick, R. J. (1995) Congenital erythropoietic porphyria: identification and expression of 10 mutations in the uroporphyrinogen III synthase gene. *J. Clin. Invest. 95*, 905–912.
9. Lazebnik, N., and Lazebnik, R. S. (2004) The prenatal presentation of congenital erythropoietic porphyria: report of two siblings with elevated maternal serum alpha-fetoprotein. *Prenatal Diagn. 24*, 282–286.
10. Wiederholt, T., Poblete-Gutierrez, P., Gardlo, K., Goerz, G., Bolsen, K., Merk, H. F., and Frank, J. (2006) Identification of mutations in the uroporphyrinogen III cosynthase gene in German patients with congenital erythropoietic porphyria. *Physiol. Res. 55*, S85−92.
11. Berry, A. A., Desnick, R. J., Astrin, K. H., Shabbeer, J., Lucky, A. W., and Lim, H. W. (2005) Two brothers with mild congenital erythropoietic porphyria due to a novel genotype. *Arch. Dermatol. 141*, 1575–1579.
12. To-Figueras, J., Badenas, C., Mascaro, J. M., Madrigal, I., Merino, A., Bastida, P., Lecha, M., and Herrero, C. (2007) Study of the genotype-phenotype relationship in four cases of congenital erythropoietic porphyria. *Blood Cells Mol. Dis. 38*, 242–246.
13. Omata, Y., Sakamoto, H., Higashimoto, Y., Hayashi, S., and Noguchi, M. (2004) Purification and characterization of human uroporphyrinogen III synthase expressed in Escherichia coli. *J. Biochem. 136*, 211–220.
14. Godoy-Ruiz, R., Ariza, F., Rodriguez-Larrea, D., Perez-Jimenez, R., Ibarra-Molero, B., and Sanchez-Ruiz, J. M. (2006) Natural selection for kinetic stability is a likely origin of correlations between mutational effects on protein energetics and frequencies of amino acid occurrences in sequence alignments. *J. Mol. Biol. 362*, 966–978.
15. Baker, D., and Agard, D. A. (1994) Kinetics versus thermodynamics in protein folding. *Biochemistry 33*, 7505–7509.
16. Duy, C., and Fitter, J. (2005) Thermostability of irreversible unfolding alpha-amylases analyzed by unfolding kinetics. *J. Biol. Chem. 280*, 37360–37365.
17. Perera, S., and Bapat, B. (2008) The MLH1 variants p.Arg265Cys and p.Lys618Ala affect protein stability while p.Leu749Gln affects heterodimer formation. *Hum. Mutat. 29*, 332.
18. Rodriguez-Larrea, D., Minning, S., Borchert, T. V., and Sanchez-Ruiz, J. M. (2006) Role of solvation barriers in protein kinetic stability. *J. Mol. Biol. 360*, 715–724.
19. Wang, Y., Scott, C. R., Gelb, M. H., and Turecek, F. (2008) Direct assay of enzymes in heme biosynthesis for the detection of porphyrias by tandem mass spectrometry. Porphobilinogen deaminase. *Anal. Chem. 80*, 2606–2611.
20. Shoolingin-Jordan, P. M., and Leadbeater, R. (1997) Coupled assay for uroporphyrinogen III synthase. *Methods Enzymol. 281*, 327–336.
21. Gill, S. C., and Von Hippel, P. H. (1989) Calculation of protein extinction coefficients from amino-acid sequence data. *Anal. Biochem. 182*, 319–326.
22. Tsai, S. F., Bishop, D. F., and Desnick, R. J. (1987) Coupled-enzyme and direct assays for uroporphyrinogen III synthase activity in human erythrocytes and cultured lymphoblasts. Enzymatic diagnosis of heterozygotes and homozygotes with congenital erythropoietic porphyria. *Anal. Biochem. 166*, 120–133.
23. Hart, G. J., and Battersby, A. R. (1985) Purification and properties of uroporphyrinogen III synthase (co-synthetase) from Euglena gracilis. *Biochem. J. 232*, 151–160.
24. Wayne, A. W., Straight, R. C., Wales, E. E., and Englert, E. (1979) Isomers of uroporphyrin free acids separated by HPLC. *J. High Resolut. Chromatogr. 2*, 621–622.
25. Santoro, M. M., and Bolen, D. W. (1988) Unfolding free energy changes determined by the linear extrapolation method. 1. Unfolding of phenylmethanesulfonyl alpha-chymotrypsin using different denaturants. *Biochemistry 27*, 8063–8068.
26. Zheng, G., Stait-Gardner, T., Anil Kumar, P. G., Torres, A. M., and Price, W. S. (2008) PGSTE-WATERGATE: an STE-based PGSE NMR sequence with excellent solvent suppression. *J. Magn. Reson. 191*, 159–163.
27. Ged, C., Megarbane, H., Chouery, E., Lalanne, M., Megarbane, A., and de Verneuil, H. (2004) Congenital erythropoietic porphyria: report of a novel mutation with absence of clinical manifestations in a homozygous mutant sibling. *J. Invest. Dermatol. 123*, 589–591.
28. Dupuis-Girod, S., Akkari, V., Ged, C., Galambrun, C., Kebaili, K., Deybach, J. C., Claudy, A., Geburher, L., Philippe, N., de Verneuil, H., and Bertrand, Y. (2005) Successful match-unrelated donor bone marrow transplantation for congenital erythropoietic porphyria (Gunther disease). *Eur. J. Pediatr. 164*, 104–107.
29. Bishop, D. F., Johansson, A., Phelps, R., Shady, A. A., Ramirez, M. C., Yasuda, M., Caro, A., and Desnick, R. J. (2006) Uroporphyrinogen III synthase knock-in mice have the human congenital erythropoietic porphyria phenotype, including the characteristic light-induced cutaneous lesions. *Am. J. Hum. Genet. 78*, 645–658.
30. Tezcan, I., Xu, W., Gurgey, A., Tuncer, M., Cetin, M., Oner, C., Yetgin, S., Ersoy, F., Aizencang, G., Astrin, K. H., and Desnick, R. J. (1998) Congenital erythropoietic porphyria successfully treated by allogeneic bone marrow transplantation. *Blood 92*, 4053–4058.
31. Warner, C. A., Yoo, H. W., Roberts, A. G., and Desnick, R. J. (1992) Congenital erythropoietic porphyria: identification and expression of exonic mutations in the uroporphyrinogen III synthase gene. *J. Clin. Invest. 89*, 693–700.
32. Cunha, L., Kuti, M., Bishop, D. F., Mezei, M., Zeng, L., Zhou, M. M., and Desnick, R. J. (2007) Human uroporphyrinogen III synthase: NMR-based mapping of the active site. *Proteins 71*, 855–873.
33. Becktel, W. J., and Schellman, J. A. (1987) Protein stability curves. *Biopolymers 26*, 1859–1877.
34. Plaza del Pino, I. M., Ibarra-Molero, B., and Sanchez-Ruiz, J. M. (2000) Lower kinetic limit to protein thermal stability: a proposal regarding protein stability in vivo and its relation with misfolding diseases. *Proteins 40*, 58–70.
35. Miles, C. A., Burjanadze, T. V., and Bailey, A. J. (1995) The kinetics of the thermal denaturation of collagen in unrestrained rat tail tendon determined by differential scanning calorimetry. *J. Mol. Biol. 245*, 437–446.

36. Sanchez-Ruiz, J. M., Lopez-Lacomba, J. L., Cortijo, M., and Mateo, P. L. (1988) Differential scanning calorimetry of the irreversible thermal denaturation of thermolysin. *Biochemistry 27*, 1648–1652.
37. Tello-Solis, S. R., and Hernandez-Arana, A. (1995) Effect of irreversibility on the thermodynamic characterization of the thermal denaturation of Aspergillus saitoi acid proteinase. *Biochem. J. 311*, 969–974.
38. Mathews, M. A., Schubert, H. L., Whitby, F. G., Alexander, K. J., Schadick, K., Bergonia, H. A., Phillips, J. D., and Hill, C. P. (2001) Crystal structure of human uroporphyrinogen III synthase. *EMBO J. 20*, 5832–5839.
39. Frank, J., Wang, X., Lam, H. M., Aita, V. M., Jugert, F. K., Goerz, G., Merk, H. F., Poh-Fitzpatrick, M. B., and Christiano, A. M. (1998) C73R is a hotspot mutation in the uroporphyrinogen III synthase gene in congenital erythropoietic porphyria. *Ann. Hum. Genet. 62*, 225–230.
40. Fontanellas, A., Bensidhoum, M., Enriquez de Salamanca, R., Moruno Tirado, A., de Verneuil, H., and Ged, C. (1996) A systematic analysis of the mutations of the uroporphyrinogen III synthase gene in congenital erythropoietic porphyria. *Eur. J. Hum. Genet. 4*, 274–282.

BI801731Q